Study of Neutron Structure with Spectator Tagging via $eD \rightarrow e'NX$ in MEIC

Kijun Park [1]

[1]Old Dominion University/Jefferson Lab

March 9, 2015

Electron Ion Collider

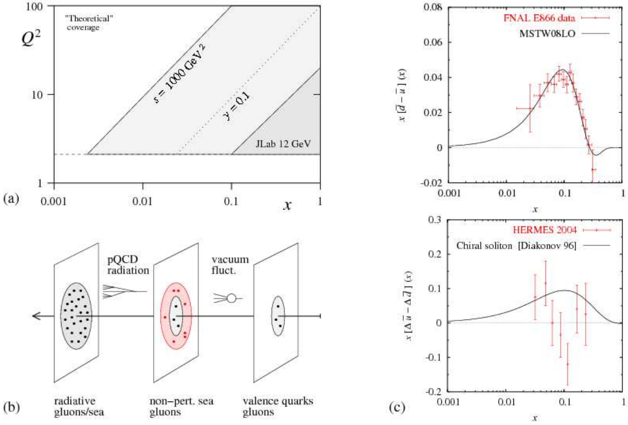

- Importance of low x physics
  - Gluon and sea quark (transverse) imaging of the nucleon
  - Nucleon Spin (ΔG vs. log Q^2, transverse momentum)
  - Nucleon QCD (gluons in nuclei, quark/gluon energy loss)
  - QCD vacuum and Hadron Structure and formation

Electron Ion Collider → Spectator Tagging

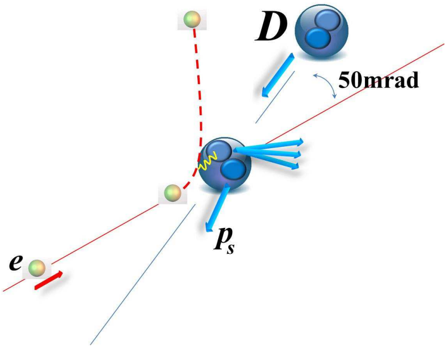

Figure : A Schematic of Reaction $eD \to e' p_s X$

- No Free Neutron Target
  - Neutron Structure (flavor decomposition of quark spin, sea quarks, gluon pol.)
  - Spectator Nucleon Tagging (forward detection/unique for collider)
  - Polarized Deuterium (a simple wave function/pol. neutron spin/limited FSI/coherence $N = 2, \ldots$)

Spectator Tagging → Extrapolating Neutron Structure

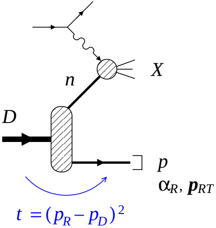

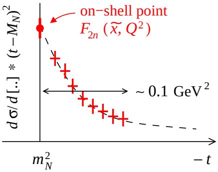

[by courtesy of C. Weiss]

- Light-Cone momentum fraction, Transverse momentum of recoil proton:

$$\alpha_R = 2\frac{E_R + p_R^z}{M_D}, \quad \vec{p}_{RT}$$

- Cross-section in the IA

$$\frac{d\sigma}{dxdQ^2 d\alpha_R d^3p_R/E_R} = f_{Flux} \times S_D(\alpha_R, p_{RT}) \times F_{2n}\left(\frac{x}{2-\alpha_R}, Q^2\right)$$

- On-shell extrapolation: $t \to M_N^2 \quad (t - M_N^2 \equiv t' \to 0)$
  - Free neutron structure at pole
  - FSI does not affect to pole value
  - Model-independent method

Spectator Tagging: Coherent Effects at $x \ll 0.1$

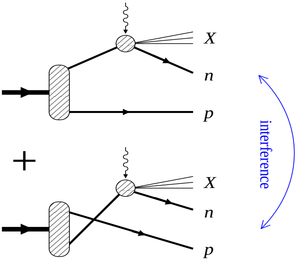

- Shadowing effect important in inclusive DIS $x \ll 0.1$
- Diffractive scattering on single nucleon
- Interference between scattered p and n

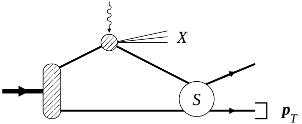

- Shadowing in Tagged DIS
- Coherent effect is clean ($N = 2$)
- Systematics is important (unpol./pol.) in p-n
- FSI between p and n $\rightarrow$ distortion of p_T, spin

[by courtesy of C. Weiss]

Far-forward Detection in EIC

- Good acceptance for all ion fragments - rigidity different from beam
  - Large magnet apertures (small gradients a fixed maximum peak field)
- Good acceptance for low-p_T recoils - rigidity similar to beam
  - Small beam size detection point (downstream focus, efficient cooling)
  - Large dispersion (generated after the IP, $D{=}D'{=}0$ the IP)
- Good momentum and angular resolution
  - Longitudinal $dp/p \approx 4 \cdot 10^{-4}$
  - Angular in θ, for all ϕ: $\approx$ 0.2mrad
  - $p_{RT} \approx$ 15MeV/c resolution for tagged nucleon in 100GeV deuterium beam
  - Long, instrumented drift space (no apertures, magnet, ...)
- Sufficient beam line separation ($\approx$ 1m)

MC Simulation

Basic configuration:

- $E_e = 5$ GeV, $E_D = 100$ GeV, $p_R < 300$ MeV, cross-angle: 50 mrad
- Normal. Emittances: $dp/p = 3 \times 10^{-4}$, $d\theta = 2 \times 10^{-4}$,
- Luminosity$= 10^{33}\mathrm{cm}^{-2}\mathrm{sec}^{-1}$, Time$= 10^{6}(\mathrm{sec})$, [e.g: HERA config.]
- User inputs: cross-section model
  - nucleon Struc.Func./deuteron Wav.Func./deuteron Residue Spect.Func.

Known facts:

- Initial State Smearing (ISS) is $\ll \pm 1\%$
- Intrinsic MC Statistical Uncertainty is $\leq 1\%$
- Sufficient t' resolution for the extrapolation
- F_{2D} structure function on-shell extrapolation with experimental uncertainty estimation

$$\Delta\sigma_{MC} = \sum N_i \Delta t' \frac{d\sigma}{dx dQ^2 dt'} \Gamma \cdot J/N_0 \ , \ count = L \cdot T \cdot \Delta\sigma_{MC} \ , \ \sigma(\Delta\sigma_{MC}) = \frac{\Delta\sigma_{MC}}{\sqrt{count}} = \sqrt{\frac{\Delta\sigma_{MC}}{L \cdot T}}$$

MC Simulation → $F_{2D}(x, Q^2, \alpha_R, t')$

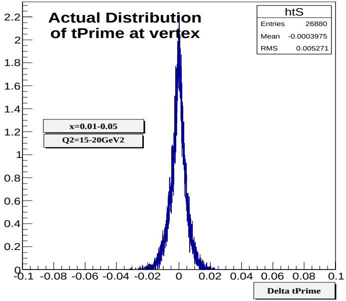

- Intrinsic momentum spread in **Ion beam** smears recoil momentum
- Dominant uncertainty for MEIC
- Effect on t' (angular spread)
- Smearing $< t'$ bin-size

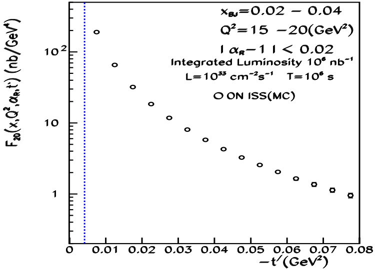

- F_{2D} vs. t' : take out f_{Flux}
- α_R : cut around 1.0 ± 0.02
- Excellent resolution allows to reach smaller t'
- Feasible on-shell extrapolation
- blue vertical dash line: $t'_{min} = 0.00416$ GeV^2

Sample Tracks in Detector Simulation

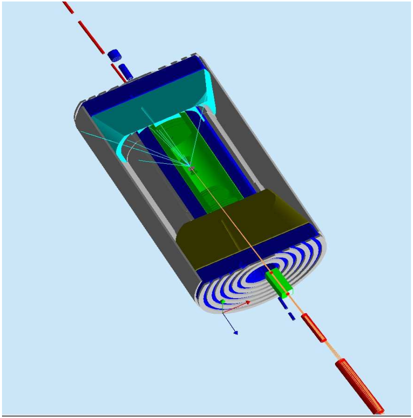

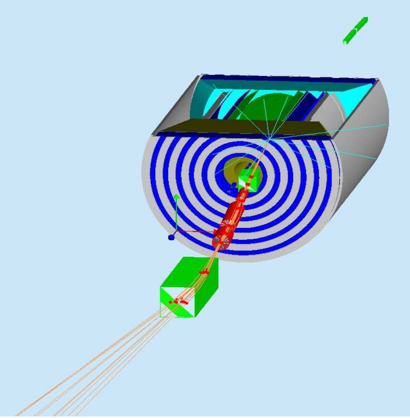

Figure : Examples of 10 physics events from $eD \rightarrow e' p_s X$, red color rays: spectator protons, light-blue rays: scattered electrons. This configuration has no solenoid field.

Polarization ($\vec{e}, \vec{D}$), *hel* $= \pm 1$ along each beam

- Asymmetry $\left(A_{||} = \frac{N_+ - N_-}{N_+ + N_-}\right)$ and A_1 $(= A_{||}/D')$, $\delta A = \sqrt{\frac{1-A^2}{N_+ + N_-}}$
- $D' = \frac{1-\epsilon}{y}\left(2 - y\left[1 + \frac{y \cdot \gamma_s}{2}\right]\right)$: Depolarization, or $\left(= \frac{(1-\epsilon)(2-y)}{y(1+\epsilon R)}\right)$

, where $\gamma_s = 4x_D^2 M_D^2/Q^2$, $y = Q^2/x_D/(s_{eD} - M_D^2)$, $R = \sigma_L/\sigma_T$

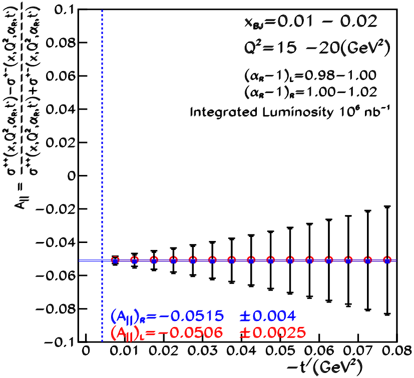

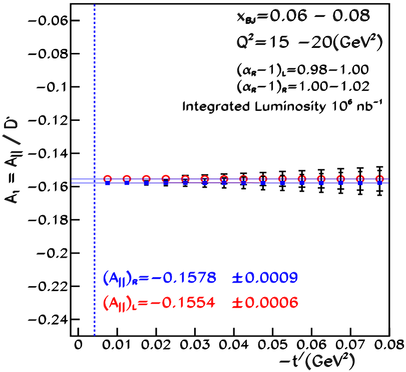

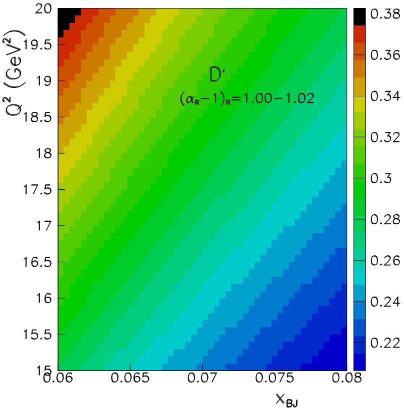

- Simple Check with certain variables at $x_{BJ} = 0.06 - 0.08$, $Q^2 = 15 - 20$ GeV^2
- $D' = \frac{1-\epsilon}{y}\left(2 - y\left[1 + \frac{y \cdot \gamma_s}{2}\right]\right)$
- $\gamma_s = 4x_D^2 M_D^2 / Q^2$,
  $y = Q^2 / x_D / (s_{eD} - M_D^2)$
- **D' in given x_{BJ}, Q^2 bins**

Diffractive Effects

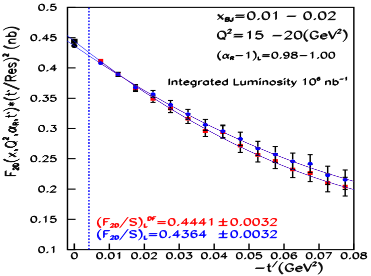

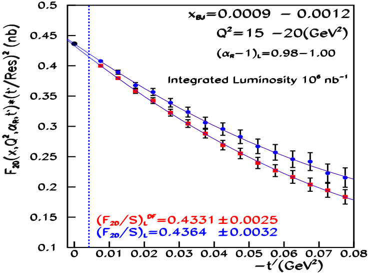

- **Kinematics I**: $x_{BJ} = 0.01 - 0.02$, $Q^2 = 15 - 20$ GeV^2
- Diffractive Effect shows a stronger impact in large t' than low
- -9%, $t' = 0.08$ GeV^2 $+1\%$, $t' = 0.01$ GeV^2

- **Kinematics II**: $x_{BJ} = 0.0009 - 0.0012$, $Q^2 = 15 - 20$ GeV^2
- Diffractive Effect shows a stronger impact in smaller x_{BJ}
- -19%, $t' = 0.08$ GeV^2 and -1.8%, $t' = 0.01$ GeV^2

[Vadim's shadowing corrections]

Systematic uncertainty: momentum smearing effect

x_{BJ} =0.04-0.06, Q^2 =30-40 GeV^2, S_{eD} =2002.442 GeV^2

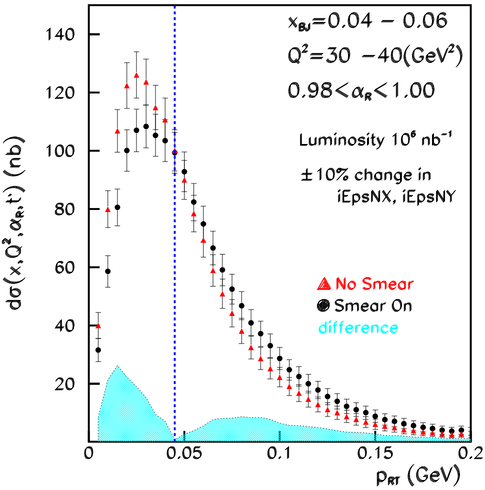

- Exact calculation (Red) and nominal smearing (Black)
- Up to 30% difference at lower p_{RT}
- Fixed Point $p_{RT} = 0.45 GeV$ (vertical dashed line)
- Difference between no-smearing and nominal smearing of Ion beam Trans. emittances

Global systematic uncertainty: p_{RT} smearing

x_{BJ} =0.0499-0.0501, Q^2 =34.99-35.01 GeV^2

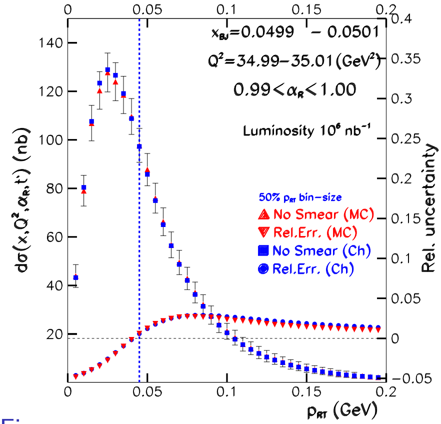

Figure : Using correct p_{RT} definition in the collinear frame.

- The systematic uncertainty from the uncertainty in the beam rms is $\pm 2.5\%$
- Check the relation between t' and p_{RT} in Code (make sure print out same values)
- $|\vec{P_R}|^2 = \frac{-t'}{2}\left(1 - \frac{t'}{2M_D^2}\right) + \frac{M_D^2}{4} - M_N^2$, where $t' = M_N^2 - t$
- $\vec{P_{RT}} = \sqrt{|\vec{P_R}|^2 - pSpec\_Rest_z^2} = invts.pPerpS$
- Relative Error (Rel.Err.)

$$= \frac{\left(\frac{d\sigma}{dxdQ^2,..,p_R^{nom+\delta}}\right) - \left(\frac{d\sigma}{dxdQ^2,..,p_R^{nom}}\right)}{\left(\frac{d\sigma}{dxdQ^2,..,p_R^{nom}}\right)}$$

** Random number seed is randomized each run, the ran.num.seed error $\ll 1\%$

$F_{2D}\cdot Spec(RES,(t')^2)$ as a function of t'

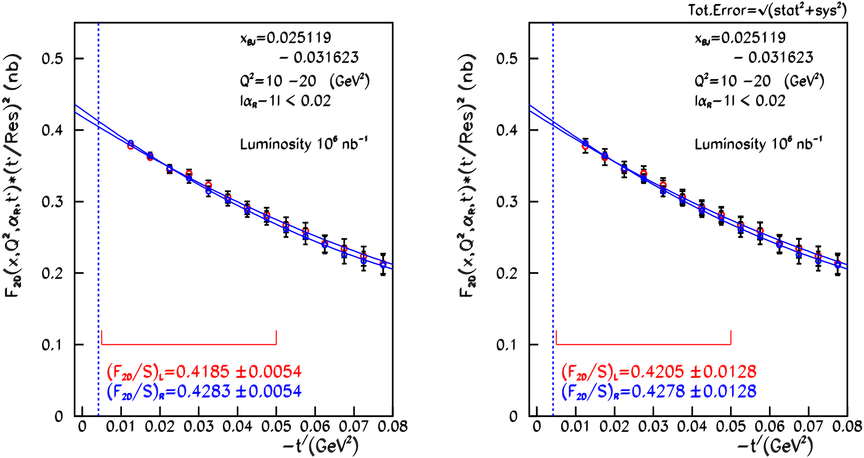

- Systematic uncertainty is dominated at lower t'
- On-shell extrapolation is about 0.5% change
- Extrapolation fitting uncertainty gets larger factor of $\sim$2.4

- $E_e = 5$ GeV, $E_D = 100$ GeV, $s_{eD} = 2002.442$ GeV^2
- $L = 10^{33} cm^{-2} s^{-1}$, $T = 3 \times 10^6 s$

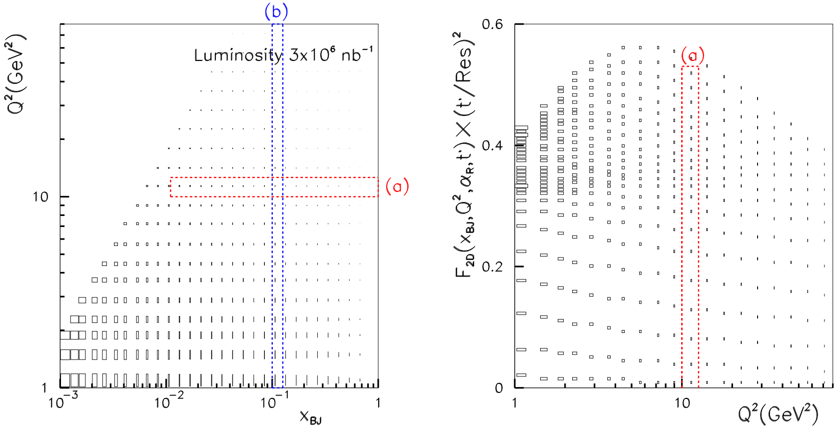

Figure : (Left) Kinematic map of F_{2n} ($\hat{z}$-axis) in terms of x_{BJ}, Q^2, (right) F_{2n} vs. Q^2. Band-(a): x_{BJ} dependence at fixed $Q^2 = 10.0 - 12.58$ GeV^2, band-(b): Q^2 dependence at fixed $x_{BJ} = 0.1 - 0.126$

Extrapolation F_{2n}: x_{BJ}-dependence at fixed $\langle Q^2 \rangle = 11.29\text{GeV}^2$

Kinematic Band-(a)

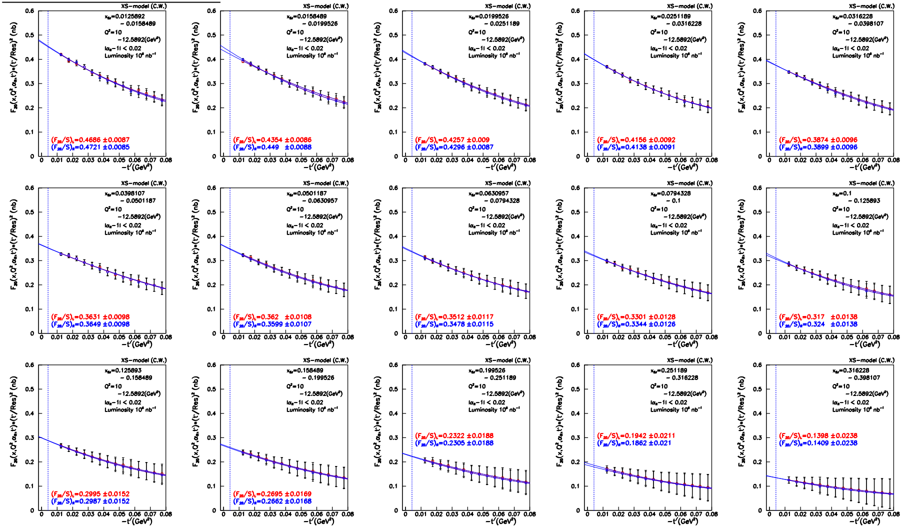

On-shell extrapolation F_{2n} vs. x_{BJ} at fixed $\langle Q^2 \rangle = 11.29\text{GeV}^2$

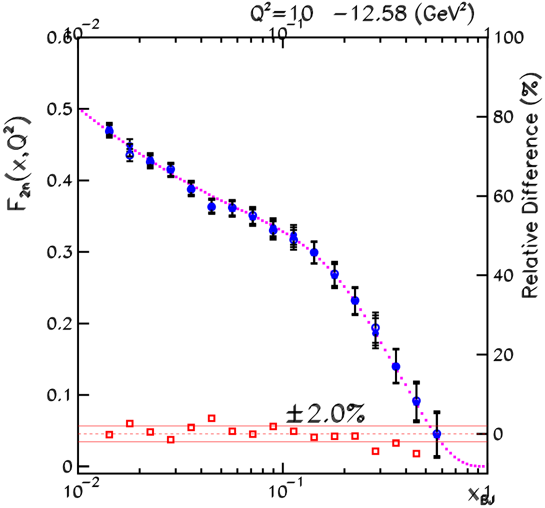

Figure : **Magenta dots**: F_{2n} model input, **Blue solid/open circles**: extrapolation (two α_R bins) from MC, **Red open boxes**: the relative difference ($\delta F_{2n}/F_{2n}$) of the result from the input at center of bin

Extrapolation F_{2n}: Q^2-dependence at fixed $\langle x_{BJ} \rangle = 0.1129$

Kinematic Band-(b)

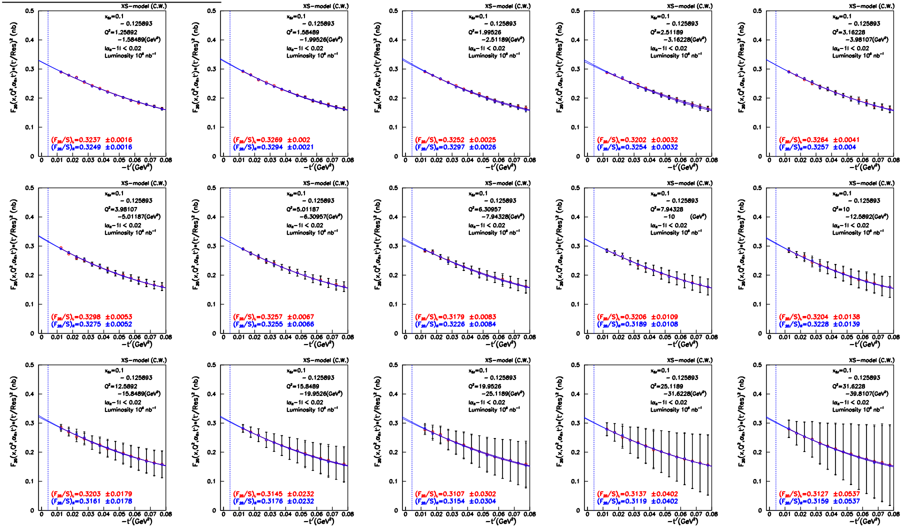

On-shell extrapolation F_{2n} vs. Q^2 at fixed $\langle x_{BJ} \rangle = 0.1129\text{GeV}^2$

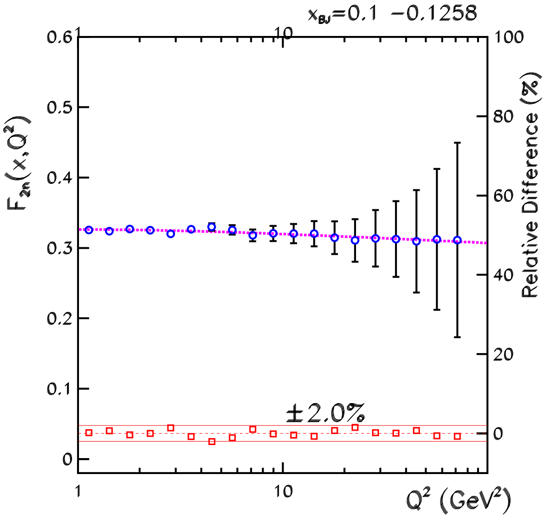

Figure : **Magenta dots**: F_{2n} model input, **Blue open circles**: extrapolation (averaged) from MC, **Red open boxes**: the relative difference ($\delta F_{2n}/F_{2n}$) of the result from the input at center of bin

Kinematic Band-(a)

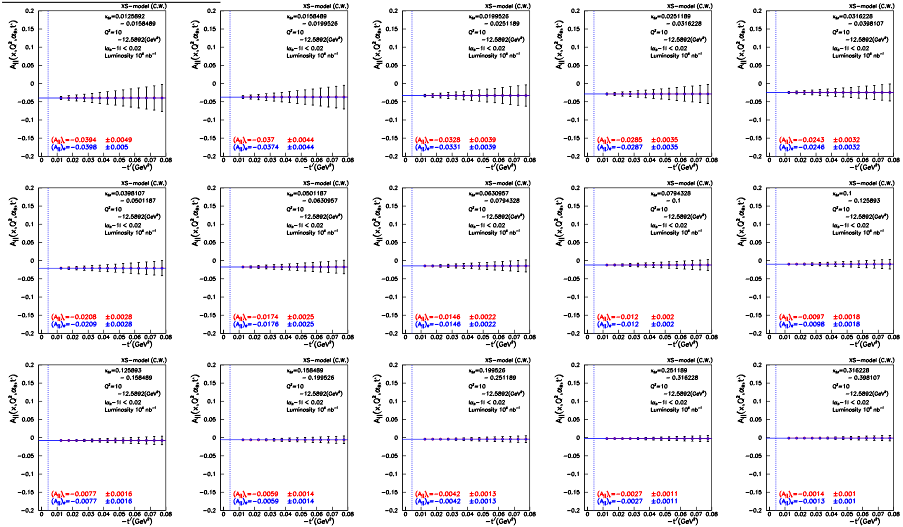

On-shell extrapolation $A_{||}$ vs. x_{BJ} at fixed $\langle Q^2 \rangle = 11.29\text{GeV}^2$

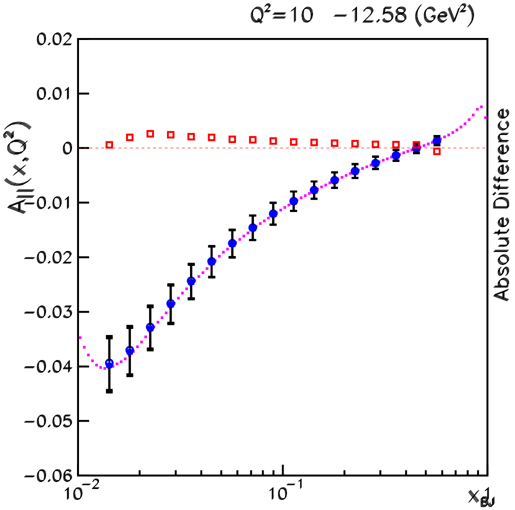

Figure : **Magenta dots**: $A_{||}$ model input, **Blue solid/open circles**: extrapolation (two α_R bins) from MC, **Red open boxes**: the absolute difference ($\delta A_{||}$) of the result from the input at center of bin

On-shell extrapolation $A_{||}$ vs. Q^2 at fixed $\langle x_{BJ} \rangle = 0.1129$

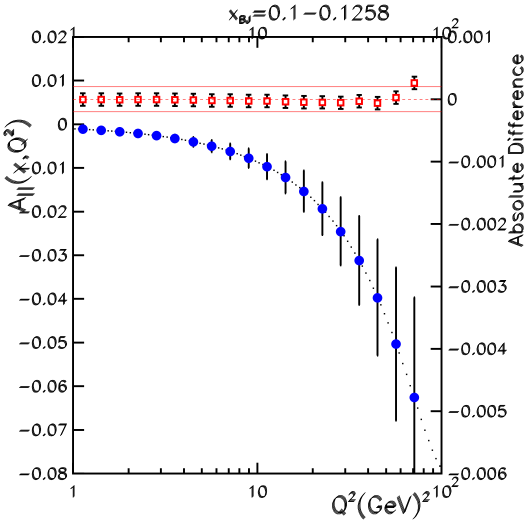

Figure : **Black dots**: $A_{||}$ model input, **Blue solid/open circles**: extrapolation (two α_R bins) from MC, **Red open boxes**: the absolute difference ($\delta A_{||}$) of the result from the input at center of bin

Summary

- Established the MC simulation with EIC configuration
- On-shell extrapolation of F_{2n} & $A_{||}$ have been obtained
- Overall 1% level of statistical uncertainty, Dominant uncertainty is the Systematics
- Global systematic uncertainty $\delta\sigma/\sigma = 2.5\%$, $\delta A/A = 1.7\%$
  Point-to-point systematic uncertainty (Gaussian randomization) $\sim$ 0.5%
- Looking forward to seeing what pseudo-data can guide for the global fits

BACKUP SLIDE

Thank you for your attention !

Systematic uncertainty: Collider/Collinear

- pin down with a very narrow kinematic region
- x_{BJ} =0.0499-0.0501, Q^2 =34.9-35.1 GeV^2, S_{eD} =2002.442 GeV^2, $|\alpha_R - 1| < 0.01$
- $\delta p_x = p_{D_x}^{Norm} - p_{D_x}^{Smear}$ at Collider and Collinear

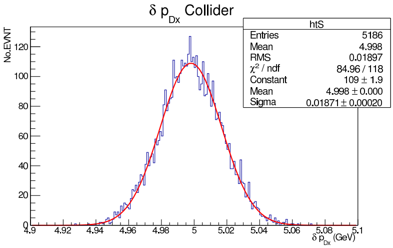

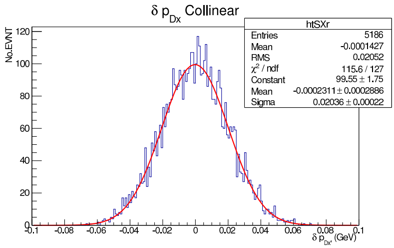

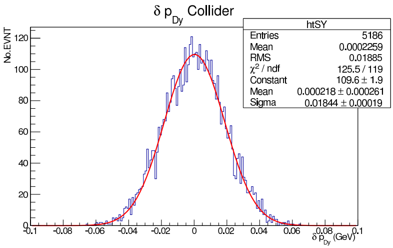

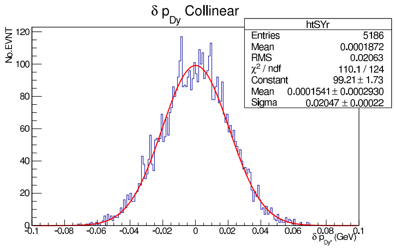

Comparison of pseudo-data: S.Kuhn vs. C.Weiss

- Beams : $E_e = 5$ GeV, $E_d = 100$ GeV
- Kinematics : $x_{BJ} = 0.02 - 0.04$, $Q^2 = 15 - 20$ GeV^2

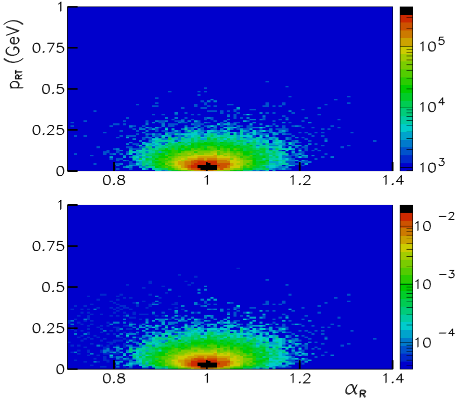

1D : p_{RT} and α_R (S.Kuhn)

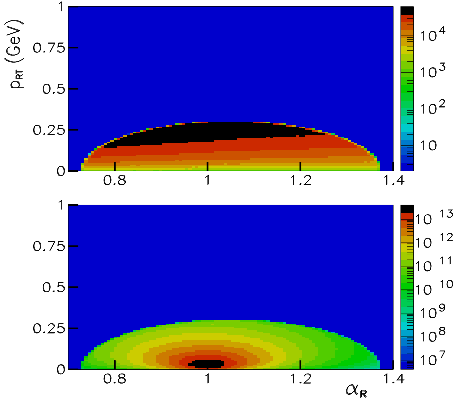

p_{RT} vs. α_R (C.Weiss)

Cross-sections: S.Kuhn vs. C.Weiss

Beams : $E_e = 5$ GeV, $E_D = 100$ GeV
Kinematics : $x_{BJ} = 0.02 - 0.04$, $Q^2 = 15 - 20$ GeV^2

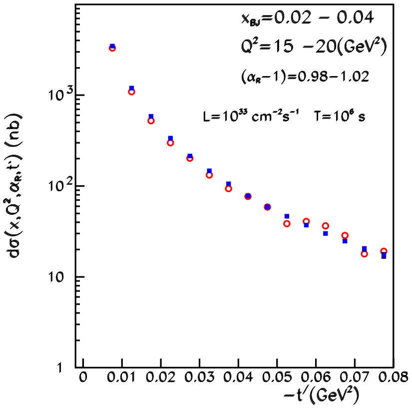

cross-section comparison as function of t'

- blue : MC data using C. Weiss model
- red : S.Kuhn MC data using C. Weiss model

On-shell extrapolation F_{2n}: models

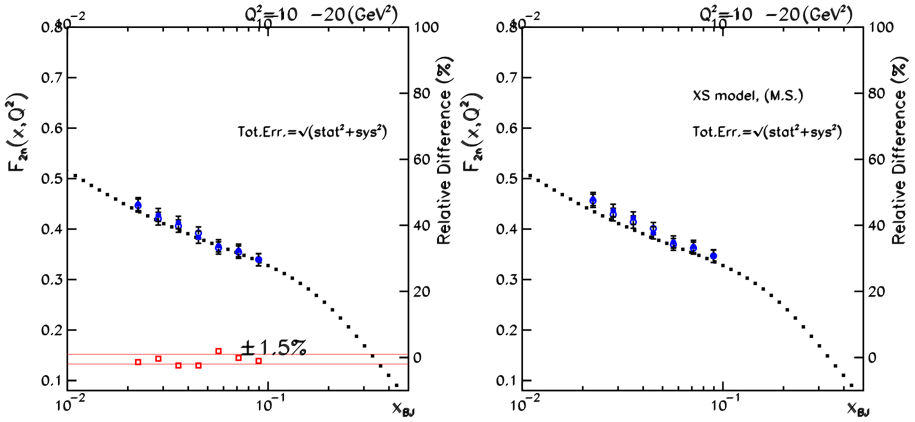

Figure : On-shell extrapolation of F_{2n} using C.W. (left) and M.S. (right)

- Cross-section model : M. Sargsian (M.S.)
  Cross-section difference with C. Weiss (C.W.) $\sim$ 4%
  On-shell extrapolation difference with C.W. $\sim$ 2%
- M.S. cross-sections are expected lower than one of C.W. model due to *D*-state (??%)
- extrapolation is larger because ...

A Sample Kinematic Region

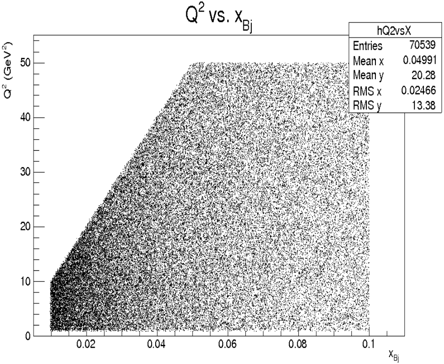

Figure : Kinematic coverage: Q^2 vs. x_{BJ} at given MEIC configuration

- $E_e = 5$ GeV, $E_D = 100$ GeV
  $s_{eD} = 2002.442$ GeV^2
- $\frac{d\sigma}{dx_{BJ}dQ^2\ldots} \cdot F_{spec}$ as a function t'
  where is $t' = M_N^2 - t$
- Various x_{BJ} bins from 0.02 to 0.1 at fixed Q^2 =10-20 GeV^2

x_{BJ}	x_{BJ}^{MIN}	x_{BJ}^{MAX}	Δx_{BJ}
1	0.01995	0.02512	0.00517
2	0.02512	0.03162	0.00651
3	0.03162	0.03981	0.00819
4	0.03981	0.05012	0.01031
5	0.05012	0.06309	0.01297
6	0.06309	0.07943	0.01634
7	0.07943	0.10000	0.02057

$F_{2D} \cdot \mathrm{Spec}(RES, (t')^2)$ as a function of t'

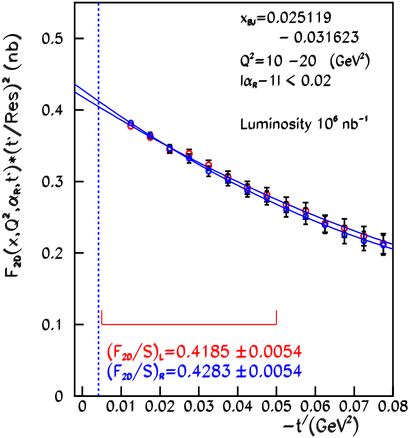

Figure : Examples: on-shell extrapolation of F_{2n} for two x_{BJ} bins with α cuts. $\alpha_R - 1 = 0.98 - 1.00$: $(F_{2D}/S)_L$, $\alpha_R - 1 = 1.00 - 1.02$: $(F_{2D}/S)_R$

On-shell extrapolation of neutron structure function

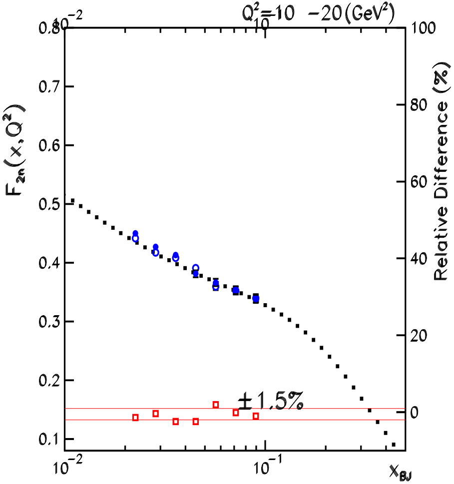

Figure : On-shell extrapolation of F_2^n from MC vs. input

- x_{BJ} = 0.02 - 0.1, Q^2 = 10 - 20 GeV^2
- (black-dotted) C.Weiss' cross-section model
- Extrapolation from fit to on-shell point

  α_R=0.98-1.00(solid),
  α_R=1.00-1.02(open)
- (Red open boxes) Relative differences
- Statistical uncertaity only

Systematic uncertainty: extrapolation

- Relative systematic uncertainty from smearing $\delta\sigma/\sigma = 0.1$
- $\frac{d\sigma}{dx_{BJ}dQ^2\ldots} \cdot F_{spec}$ as a function t', where is $t' = M_N^2 - t$
- Converting between t' and p_R is followed by Eq.(35) from C.Weiss' note ("tag.pdf")
- total uncertainty $= \sqrt{\delta^2_{\mathrm{stat}} + \delta^2_{\mathrm{sys}}}$
- No data randomization taken into account in this step
  However, this effect is $\sim 1\%$

x_{BJ} bin	RMS wid.(α_{left})	RMS wid.(α_{right})
1	0.0062	0.0062
2	0.0064	0.0065
3	0.0070	0.0068
4	0.0072	0.0071
5	0.0074	0.0077
6	0.0078	0.0079
7	0.0086	0.0086

** RMS Width of $(F_{2D} - F_{2D}^{extract})/F_{2D}$

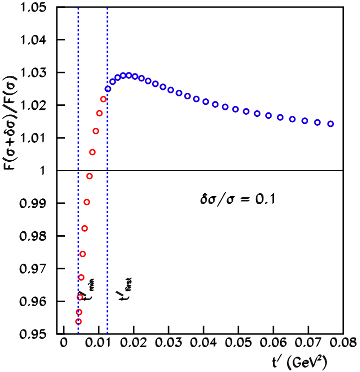

Figure : $t'_{min} = 0.00416$ GeV^2 ($\sim p_{RT} = 0$ GeV), $t'_{first} = 0.0125$ GeV^2 is the first t' bin that we can access experimentally within finite t' resolution & α_R bin